Journal of Materials and Environmental Science
ISSN : 2028-2508
CODEN : JMESCN

J. Mater. Environ. Sci., 2026, Volume 17, Issue 6, Page 979-990

http://www.jmaterenvironsci.com

Laboratory study of flow interaction with obstacle configuration

Youssef M.[1,2], Amel S.[1*], Azeddine K.[2].

[1] *University of Carthage, National Agronomic Institute of Tunisia (INAT), Laboratory GREEN-TEAM; LR17AGR01, Tunis, 1002, Tunisia*

[2] *University of Orleans, INSA-CVL, PRISME, Orleans, France*

**Corresponding Author Email: amel.inat@hotmail.fr*

Received *08 April 2026,*
Revised *15 June 2026,*
Accepted *17 June 2026*

Keywords:

- ✓ *Open-channel flow,*
- ✓ *Obstacle configuration,*
- ✓ *Water surface profile,*
- ✓ *Flow–structure interaction.*

Citation*: Youssef M., Amel S., Azeddine K. (2026) Laboratory study of flow interaction with obstacle configuration, J. Mater. Environ. Sci., 17(6), 979-990.*

Abstract: This study presents an experimental investigation of water surface profile variations in an open-channel flow under different discharge conditions with a single obstacle configuration. Experiments were conducted in the hydraulic laboratory at INAT, University of Carthage, using a flume 10 m long, 0.80 m wide, and 0.60 m high with a 1% slope. The setup enabled precise control of boundary conditions and accurate measurement of flow depth and surface elevation. A configuration of cylindrical concrete obstacles (15 cm height, 10 cm diameter) was installed to examine its influence on water level distribution. Six steady discharges, ranging from 9.8 to 34.2 $L \cdot s^{-1}$, were applied to cover low to high flow regimes. Point gauges placed along the flume recorded surface elevations upstream, within, and downstream of the obstacle region, ensuring reproducible and reliable measurements. Results show that the obstacle configuration considerably affects the water surface profile and flow structure. A backwater rise occurs upstream, while within the obstacle region, flow disturbances and turbulence intensify with increasing discharge. Higher flow rates generate a larger kinetic energy deficit zone around the obstacles, followed by a gradual downstream recovery of the surface profile. This study provides experimental evidence of how obstacle geometry influences open-channel flow behavior, offering valuable data for validating numerical models and optimizing the design of hydraulic and river engineering structure.

1. Introduction

The interaction between water flow and obstacles is a critical topic in hydraulic engineering, as it directly affects the design and safety of hydraulic structures, such as bridge piers, weirs, and flood protection works (Oodi *et al.*, 2025, Qasim *et al.*, 2021). Understanding the influence of obstacles on water surface profiles, flow velocities, and turbulence patterns is essential for predicting hydraulic behavior in rivers and engineered channels (Mahjoub *et al.*, 2024a).

Previous studies, including numerical and simulation-based investigations, have explored the effect of obstacle configurations on water flow (Mahjoub *et al.*, 2024b, Tran, 2015). For instance, recent simulation work has demonstrated how different arrangements of bridge piers can significantly alter velocity fields and water surface elevations, highlighting regions of flow acceleration, separation, and turbulence development (Gharbi *et al.*, 2016; Al-Jubouri *et al.*, 2024; Soori *et al.*, 2026). These computational studies provide a valuable framework for understanding flow–obstacle interactions, but their results require experimental validation to capture the complexities of real water behavior under controlled physical conditions (Tran, 2015, Rasha *et al.*, 2023, Nasim *et al.*, 2018).

The present study builds on this foundation by conducting experimental investigations in a laboratory channel. A single obstacle configuration was installed to analyze its effect on the water surface profile under varying discharge conditions. Six discharges were applied, ranging from 9.2 to 35 liters per second, to observe how water levels evolve upstream, within, and downstream of the obstacle. In addition, the study examines the influence of the obstacle on flow velocity and the formation of turbulent regions, which become more pronounced with increasing discharge.

The main objective of this work is to provide an experimental characterization of water surface behavior and flow variations around an obstacle configuration. By measuring water heights and analyzing the effects of different discharges, this study aims to quantify the impact of obstacles on hydraulic behavior, validate insights from previous simulations, and provide practical information for the design and management of hydraulic structures.

2. Experimental details

2.1 Description of the laboratory channel

Experimental studies play a crucial role in hydraulic research, providing direct observation and measurement of flow behavior under controlled conditions. They complement theoretical and numerical approaches by offering accurate, real-world data that capture complex flow phenomena, including water surface variations and turbulence, which are often difficult to predict.

The experiments were conducted in the hydraulic laboratory at INAT, University of Carthage, in a flume specifically designed to investigate flow–obstacle interactions. The flume has a total length of 10 m, a width of 0.80 m, and a height of 0.60 m, with a 1% longitudinal slope, allowing the simulation of flow conditions inspired by natural watercourses. This slope helps reproduce realistic flow velocities and surface profiles similar to those observed in rivers and engineered channels. Flow was generated and regulated using four independent pumps, enabling a wide range of steady discharges from 9.2 liters per second to 35 liters per second, covering low to high flow regimes. This setup provided the flexibility necessary to systematically study the evolution of the water surface profile under different hydraulic conditions and ensured reproducibility for all experimental scenarios (**Figure 1**).

Figure 1. Overview of the experimental setup in the hydraulic laboratory.

2.2 Obstacle Configuration and Creation

To study the influence of obstacles on water surface behavior, a single configuration of cylindrical obstacles was installed in the laboratory flume. These obstacles were handmade from concrete, specifically designed to ensure sufficient weight and stability so that they could remain firmly in place during the experiments without damaging the flume structure. Each obstacle measured 15 cm in height and 10 cm in diameter, forming a controlled and reproducible obstruction to the flow.

During fabrication, PVC material was used as a permanent mold to shape the cylinders. The PVC casing was deliberately left in place after the concrete had solidified to provide a smooth surface finish at the water–obstacle interface. This design choice was made to minimize additional turbulence or flow disturbances that could arise from surface roughness and to ensure a more accurate comparison with previous numerical simulations, where the obstacle boundaries were also modeled as hydraulically smooth. This approach ensured consistency between experimental and numerical conditions, enhancing the reliability and interpretability of the results related to flow patterns, water surface elevations, and turbulence development around the obstacle configuration. A photograph illustrating the constructed cylindrical obstacles after fabrication is presented in **Figure 2**, showing their geometry and arrangement prior to installation in the channel.

Figure 2. Cylindrical concrete obstacles after fabrication using PVC molds.

The obstacles were arranged within the channel according to a regular grid pattern, with a longitudinal spacing of 20 cm and a transversal spacing of 20 cm between adjacent cylinders. This configuration was selected based on observations from the literature, notably studies such as Tran (2015), which demonstrated that such spacing effectively captures key hydrodynamic interactions between successive obstacles. Moreover, this arrangement corresponds to the configuration previously adopted in numerical simulations (Mahjoub *et al.*, 2024b, Tran, 2015, Gharbi *et al.*, 2016), ensuring consistency between experimental and computational approaches.

By leveraging this setup, we investigated the impact of cylindrical obstacle concentration (C) on flow characteristics such as velocity profiles, turbulence intensity, and pressure drop. The parameter C represents the combined influence of obstacle diameter (D) and spacing distances a_x (longitudinal) and a_γ (transversal), allowing for a quantitative evaluation of how obstacle density affects the overall flow resistance and energy distribution. These geometric relationships and spacing arrangements are illustrated in **Figure 3**, which provides a visual representation of the obstacle layout and the parameters defining the concentration (C):

$$C = \frac{D^2}{a_x a_y} \qquad \textbf{(Eqn. 1)}$$

The regular arrangement ensured uniform flow obstruction and facilitated the analysis of local variations in water surface elevation, turbulence generation, and velocity distribution. This systematic configuration minimized sidewall effects and provided a stable experimental basis for assessing obstacle-induced hydraulic behavior.

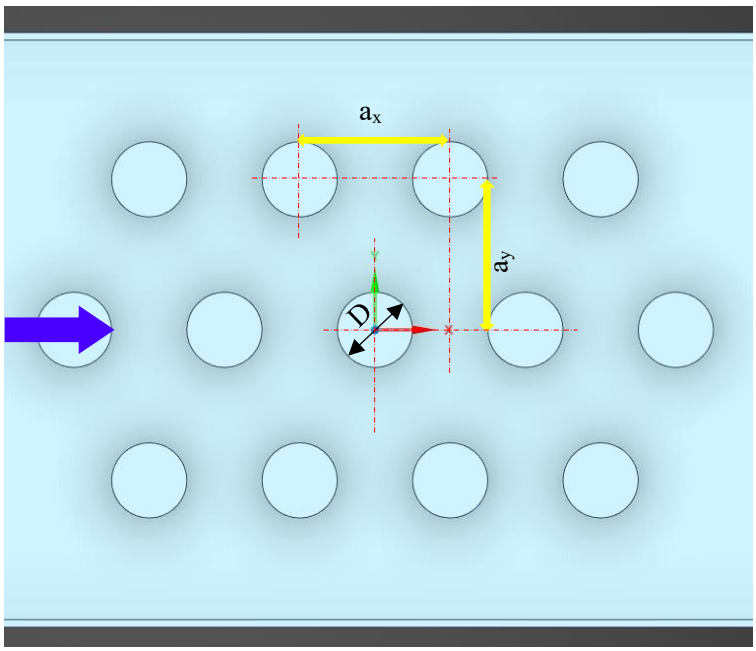

Figure 3. Geometric arrangement of cylindrical obstacles within the channel, defining the longitudinal a_x and transversal a_y spacing used to compute the obstacle concentration parameter C.

Figure 4 illustrates the spatial configuration and precise positioning of the obstacles within the channel, providing a clear representation of their geometric arrangement used in the numerical model.

Figure 4. Photograph illustrating the spatial configuration and precise positioning of the cylindrical obstacles within the experimental channel.

2.3 Methodological Framework and Governing Equations

The hydraulic behavior observed in the experimental flume is governed by the fundamental equations of fluid motion for incompressible turbulent flow, expressed by the Reynolds-Averaged Navier–Stokes (RANS) equations:

$$\rho(\frac{\partial u}{\partial t}+ u \cdot \nabla u) = -\nabla p + \nabla \cdot [\mu(\nabla u + \nabla u^{T})] + fs + fg \quad \textbf{(Eqn. 2)}$$

Here, ρ represents the fluid density, u is the velocity vector, and t denotes time. The term p corresponds to the pressure, while μ is the fluid dynamic viscosity, characterizing its resistance to shear or flow. The term fs accounts for surface tension forces, which are significant at interfaces between two fluids, and fg represents gravitational body forces acting on the fluid (Rasha *et al.*, 2023).

Together with the continuity equation:

$$\frac{\partial \rho}{\partial t}+ \nabla \cdot (\rho u) = 0 \quad \textbf{(Eqn. 3)}$$

Where ρ is the fluid density, and u is the mean velocity vector.

These equations describe the balance between inertial, pressure, viscous, and gravitational forces. In the present study, variations in discharge directly influence the relative dominance of these terms.

To quantify flow characteristics, dimensionless parameters were employed. The Reynolds number ($Re = \frac{UD}{\upsilon}$) characterizes turbulence intensity (Nasim *et al.*, 2018, Schlömer and Herget, 2023, Larsen *et al.*, 2016), while the Froude number ($Fr = \frac{U}{\sqrt{gh}}$) assesses the relative importance of inertial versus gravitational forces (Gharbi *et al.*, 2016, Nasim *et al.*, 2018, Schlömer and Herget, 2023). The obstacle concentration parameter ($C = \frac{D^2}{a_x a_y}$, **Figure 3**) represents the combined effect of obstacle diameter and spacing, linking geometric arrangement to flow resistance and energy distribution.

Complementing the RANS framework, the Bernoulli equation provides an energy-based interpretation of the observed water surface elevations:

$$\frac{P}{g\rho}+\frac{U^2}{2g}+ Z = constant \quad \textbf{(Eqn. 4)}$$

Where P is the local pressure, U the velocity, Z the elevation, ρ the fluid density, and g the gravitational acceleration. Variations in water surface elevation upstream and within the obstacle region reflect the conversion between velocity head and pressure/elevation head, with higher discharges amplifying inertial effects and generating turbulent (Rasha *et al.*, 2023, Nasim *et al.*, 2018, Schlömer and Herget, 2023), energy-deficient zones.

The combination of RANS-based momentum analysis and the Bernoulli energy perspective provides both quantitative and intuitive insight into flow dynamics (Nasim *et al.*, 2018, Larsen *et al.*,

2016), linking observed surface profiles and turbulence patterns to theoretical expectations. These relationships are further illustrated in Section 3, where experimental results are analyzed in terms of velocity distribution, turbulence evolution, and surface elevation profiles.

3. Results and Discussion

Measurements of water surface elevations and flow characteristics were performed at three representative locations along the obstacle configuration: the upstream, central, and downstream obstacles. These points capture the progressive evolution of flow behavior before, within, and after the obstacle array. For clarity in figures and analysis, data are color-coded as blue (upstream), red (central), and green (downstream), as illustrated in **Figure 5**.

Figure 5. Photograph showing the three measurement locations along the obstacle configuration: upstream (blue), central (red), and downstream (green).

Table 1 summarizes the measured water surface elevations and the corresponding variations (ΔH) at three representative positions along the obstacle configuration (initial, middle, and final) under six discharge conditions ranging from 9.8 L/s to 34.2 L/s. For each discharge, the mean inflow velocity (U_{mean}) was determined, and the water surface elevations were measured just upstream and just downstream of each obstacle within the same configuration to calculate the elevation difference (ΔH).

This systematic measurement approach enables a detailed assessment of how flow intensity influences the hydraulic gradient and surface elevation distribution along the obstacle arrangement. These data constitute the foundation for the analysis presented below and are illustrated graphically in **Figure 6**, which depicts the evolution of ΔH with increasing discharge.

As shown in **Table 1**, the measured differences in water surface elevation (ΔH) increase consistently with discharge, highlighting the growing influence of inertial and pressure terms in the flow dynamics. At low discharges (below 16 L/s), the flow remains relatively stable, and ΔH values are small, particularly around the central obstacle, where local energy dissipation is limited. However, as the discharge rises, a significant elevation of ΔH is observed both upstream and downstream, indicating stronger backwater effects and increased turbulence intensity. According to the Bernoulli relation (**Eqn. 4**), the rise in kinetic energy associated with higher velocities (**Table 1**) induces local head losses, particularly around the obstacle region where flow separation and recirculation occur. Simultaneously, the Navier–Stokes terms in **Eqn. 2** describing viscous dissipation and momentum exchange become increasingly dominant (Aksel, 2023, Saber *et al.*, 2025), especially near the obstacle surfaces, resulting in larger gradients of velocity.

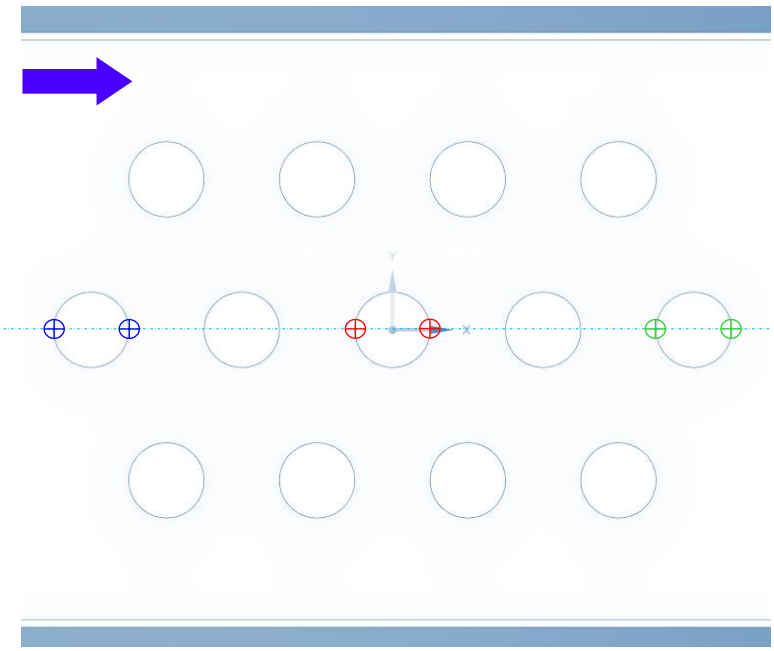

Figure 6. Measurement locations showing the upstream and downstream points of the initial, middle, and final obstacles for determining water depth variation under the same configuration and for different discharges.

Table 1. Summary of measured water surface elevations and corresponding elevation differences at the initial, middle, and final obstacles for six discharge conditions, with reference to the measurement locations shown in **Figure 6**.

	Discharge Q (l/s)	**9.8**	**16.69**	**18.5**	**26**	**28.7**	**34.2**
	U_{mean} (m/s)	**0.3**	**0.52**	**0.62**	**0.82**	**0.93**	**1.1**
Upstream obstacle	H (cm) in front	6.6	9.7	10.5	12.6	13.2	15.1
	H (cm) in back	4.6	5.6	6.2	8	8.5	10.3
	ΔH (cm)	2	4.1	4.3	4.6	4.7	4.8
Central obstacle	H (cm) in front	3.9	6.6	7.4	9.3	9.8	11.5
	H (cm) in back	3.8	5.8	6.5	8.2	8.7	9.3
	ΔH (cm)	0.1	0.8	0.9	1.1	1.1	2.2
Downstream obstacle	H (cm) in front	4.3	6.5	7.6	8.9	9.9	10.8
	H (cm) in back	0.6	1.2	2.1	3.2	3.6	3.8
	ΔH (cm)	3.7	5.3	5.5	5.7	6.3	7

These effects are clearly manifested at high discharges (above 26 L/s), where ΔH reaches its maximum values (up to 4.8 cm upstream and 7 cm downstream), reflecting a substantial redistribution of hydraulic energy. The central obstacle consistently exhibits the smallest ΔH, suggesting that it lies within a relatively balanced energy zone where opposing flow interactions partly neutralize one another.

Overall, the results demonstrate that as discharge increases, flow transitions from a quasi-laminar regime to a more turbulent one, with obstacle-induced disturbances amplifying both local energy losses and velocity fluctuations. This behavior, illustrated in **Figure 7**, confirms the theoretical expectations derived from the governing hydraulic equations.

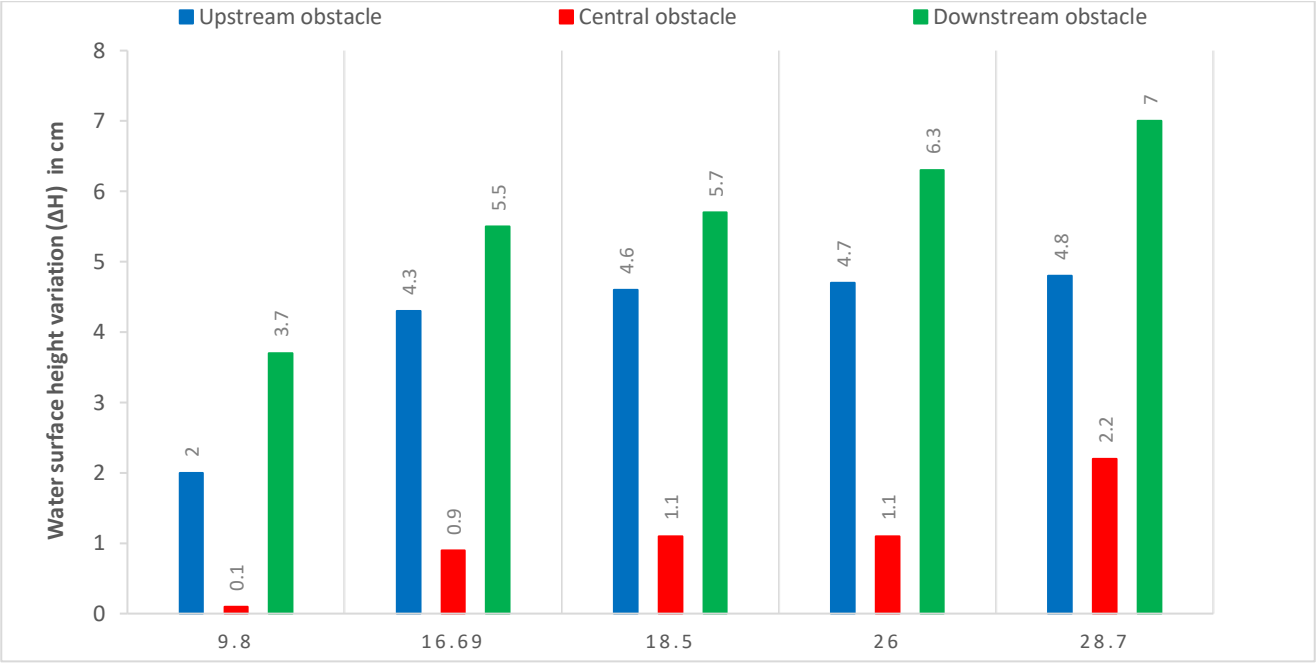

Figure 7. Water surface height variation (ΔH in cm) for each discharge (in L/s)

The obstacles create a turbulent region upstream whose length and depth increase with discharge (**Table 2**). The interaction of water with the obstacles was carefully monitored, and key parameters were measured to characterize the turbulent region upstream. These include the mean water height in the turbulent zone (H_{mean}, cm), which represents the average depth in front of the obstacles; the length of the turbulent region ($L_{turbulence}$, m), indicating the horizontal extent affected by turbulence; the maximum water height (H_{max}, cm), corresponding to the highest elevation reached in the turbulent zone; and the upstream uniform water depth ($H_{uniform}$, cm), which represents the water surface level in the absence of obstacles. All these measured parameters are reported in **Table 2**.

Table 2. Measured Flow Depths and Turbulent Zone Characteristics Upstream of Obstacles for Different Q

Q (l/s)	9.8	16.69	18.5	26	28.7	34.2
U_{mean} (m/s)	0.3	0.52	0.62	0.82	0.93	1.1
H_{mean} (cm)	4.5	6.4	7	7.8	8.7	10.4
$L_{turbulence}$ (m)	1.32	1.54	1.83	1.98	2.06	2.14
H_{max} (cm)	7.3	7.4	8.7	8.9	10.2	12.4
$H_{uniform}$ (cm)	1	2.6	2.6	3.4	3.7	3.9

At low discharges, turbulence is localized near the obstacles, with moderate mean and maximum water heights, while the upstream flow remains subcritical. As discharge increases, the turbulent zone extends further and becomes deeper, and water levels rise more markedly in front of the obstacles. The evolution of Froude and Reynolds numbers, reported in **Table 3**, reflects this transition: the flow regime shifts from subcritical at low discharge to near-critical or supercritical at higher discharge. Overall, the obstacles strongly modify the channel flow, enhancing turbulence and local water levels, and controlling the hydraulic response of the water across the full range of tested discharges.

As discharge increases from Q = 9.8 to 34.2 l/s, the flow clearly transitions from subcritical to near-critical or supercritical regimes. At the lowest discharge (Q = 9.8 l/s), the upstream uniform flow exhibits a Froude number $Fr_{upstream} \approx 0.958$ and a Reynolds number $Re_{upstream} \approx 3.00E+03$, indicating that gravitational forces dominate over inertia and the flow is mostly laminar. Within the turbulent region in front of the obstacles, the flow already shows increased mixing with Fr_turb ≈ 0.451 and $Re_{turb} \approx 1.35E+04$, reflecting localized turbulence generated by the obstacle-induced disturbance.

As discharge rises, the Froude and Reynolds numbers increase systematically. For instance, at Q = 26 l/s, the upstream flow reaches $Fr_{upstream} \approx 1.421$ and $Re_{upstream} \approx 27.9 \times 10^3$, indicating near-critical flow conditions and a dominance of inertial forces, while the turbulent region exhibits $Fr_{turb} \approx 0.939$ and $Re_{turb} \approx 6.40E+04$, demonstrating fully developed turbulence. At the highest discharge tested (Q = 34.2 l/s), $Fr_{upstream} \approx 1.777$ and $Re_{upstream} \approx 4.29E+04$, confirming supercritical upstream conditions, and the turbulent zone shows $Fr_{turb} \approx 1.089$ and $Re_{turb} \approx 1.14E+05$, highlighting the extreme turbulence and energy dissipation induced by the obstacles.

This numerical evidence is consistent with Bernoulli's principle (**Eqn. 4**): as the water accelerates over the obstacles, the increase in velocity corresponds to a rise in dynamic pressure and a reduction in potential energy, promoting turbulence. The measurements of H_{mean}, H_{max}, and $L_{turbulence}$ in **Table 2** further support this interpretation, showing that the turbulent zone becomes longer and deeper as discharge increases, reflecting the direct relationship between flow inertia (Re), flow regime (Fr), and turbulence development in the channel.

Table 3. Flow Characteristics and Turbulence Parameters Upstream of Obstacles for Varying Discharges

Q (l/s)	U_{mean} (m/s)	H_{mean} (cm)	$L_{turbulence}$ (m)	H_{max} (cm)	$H_{uniform}$ (cm)	$Fr_{upstream}$	$Re_{upstream}$	Fr_{turb}	Re_{turb}
9.8	0.3	4.5	1.32	7.3	1	0.96	3.00E+03	0.5	1.35E+04
16.69	0.52	6.4	1.54	7.4	2.6	1.03	1.35E+04	0.7	3.33E+04
18.5	0.62	7	1.83	8.7	2.6	1.23	1.61E+04	0.7	4.34E+04
26	0.82	7.8	1.98	8.9	3.4	1.42	2.79E+04	0.9	6.40E+04
28.7	0.93	8.7	2.06	10.2	3.7	1.54	3.44E+04	1	8.09E+04
34.2	1.1	10.4	2.14	12.4	3.9	1.78	4.29E+04	1	1.14E+05

Thus, the recirculation effect upstream is a key mechanism linking the obstacle-induced flow disturbance to the observed increase in both mean and maximum water heights, the extension of the turbulent region, and the shift in flow regime from subcritical to near-critical or supercritical conditions. According to the Navier–Stokes equations (**Eqn. 2**), flow separation and recirculation arise from the balance between inertial, pressure, and viscous forces. **Figures 7 and 8**, along with **Tables 2 and 3**, clearly illustrate how the size and intensity of recirculation grow systematically with discharge, reinforcing the coherent interaction between Froude and Reynolds numbers, turbulence development, and the hydraulic response of the channel.

Experimental measurements show that water surface elevations (ΔH, **Table 1**) increase systematically with discharge, with maximum upstream and downstream differences reaching 4.8 cm and 7 cm, respectively. This rise reflects the development of recirculation zones and enhanced flow separation around the obstacles, consistent with previous studies (Qasim *et al.*, 2021, Gharbi *et al.*, 2016, Rasha *et al.*, 2023). The upstream turbulent region, characterized by H_{mean}, H_{max}, $L_{turbulence}$, and $H_{uniform}$ (**Table 2**), expands in length and depth with increasing flow, indicating stronger energy dissipation and turbulence generation.

Figure 7. Evolution of Turbulent Zone Length ($L_{turbulence}$) and Mean Water Height (H_{mean}) Upstream of Obstacles for the Obstacle Configuration across Increasing Discharges

Dimensionless analyses further reveal a coherent transition: upstream Froude numbers rise from 0.96 to 1.78 and Reynolds numbers from 3.0×10^3 to 4.29×10^4, while turbulence-specific Fr_{turb} and Re_{turb} increase even more, confirming the shift from subcritical to near-critical and supercritical regimes(Mahjoub *et al.*, 2024a, Tran, 2015, Rasha *et al.*, 2023, Schlömer and Herget, 2023, Aksel, 2023, Larsen *et al.*, 2016). Overall, obstacle-induced recirculation harmoniously links water surface elevation, turbulence, and flow regime evolution, providing robust experimental validation for numerical modeling.

Conclusion

The experiments demonstrate that obstacles significantly influence flow patterns, turbulence development, and water surface profiles. Upstream water elevations (ΔH) increase with discharge, reflecting stronger backwater effects and recirculation. The turbulent zone becomes longer and deeper at higher discharges, with H_{mean}, H_{max}, and $L_{turbulence}$ directly linked to flow energy redistribution (**Table 2**).

Froude and Reynolds numbers confirm a systematic transition from subcritical to supercritical conditions, both upstream and within the turbulent zone (**Table 3**), illustrating the combined effect of inertial, gravitational, and viscous forces as described by Navier–Stokes (**Eqn. 2**) and Bernoulli (**Eqn. 4**) equations. Obstacle-induced recirculation emerges as a key mechanism controlling turbulence intensity and water surface response.

These findings validate previous numerical and experimental studies (Mahjoub *et al.*, 2024a, Gharbi *et al.*, 2016, Rasha *et al.*, 2023, Nasim *et al.*, 2018, Schlömer and Herget, 2023, Larsen *et al.*,

2016, Saber *et al.*, 2025) and provide experimental benchmarks for hydraulic structure design, flood management, and calibration of predictive models. Overall, the study highlights the tight coupling between ΔH, turbulence characteristics, and flow regime evolution, offering practical guidance for river engineering applications.

Acknowledgement

The authors extend profound gratitude to the dedicated teammate at the INAT, Madam *Hela Ben Romdhane*, whose collaborative efforts have enriched my academic journey and contributed significantly to the success of our shared endeavors.

Disclosure statement: *Conflict of Interest:* The authors declare that there are no conflicts of interest. *Compliance with Ethical Standards:* This article does not contain any studies involving human or animal subjects.

References

Aksel, M. (2023) Numerical Analysis of the Flow Structure around Inclined Solid Cylinder and Its Effect on Bed Shear Stress Distribution. *Journal of Applied Fluid Mechanics* , 16, 1627-1639. https://doi.org/10.47176/jafm.16.08.1697

Al-Jubouri M., Ray R.P., Abbas E.H. (2024). Advanced Numerical Simulation of Scour around Bridge Piers: Effects of Pier Geometry and Debris on Scour Depth. *Journal of Marine Science and Engineering*. 12(9),1637. https://doi.org/10.3390/jmse12091637

Gharbi, M., Soualmia, A., Dartus, D., & Masbernat, L. (2016). Comparison of 1D and 2D hydraulic models for floods simulation on the Medjerda Riverin Tunisia. *J. Mater. Environ. Sci*, 7(8), 3017-3026. https://www.jmaterenvironsci.com/Document/vol7/vol7_N8/315-JMES-1772-Gharbi.pdf

Larsen, B.E., Fuhrman, D.R. and Sumer, B.M. (2016) Simulation of Wave-plus-Current Scour beneath Submarine Pipelines. *Journal of Waterway , Port , Coastal , and Ocean Engineering*, 142, Article 04016003. https://doi.org/10.1061/(ASCE)WW.1943-5460.0000338

Oodi, S., Gohari, S., Di Francesco, S., Nazari, R., Nikoo, M. R., Heidarian, P., Eidi, A., & Khoshkonesh, A. (2025). Wave–Structure Interaction Modeling of Transient Flow Around Channel Obstacles and Contractions. *Water*, *17*(3), 424. https://doi.org/10.3390/w17030424

Mahjoub, Y., Soualmia, A., & Kourta, A. (2024a). Bridge Impact on Water Behavior: Simulation-Application to the Medjerda River in Tunisia. *Open Access Library Journal*, 11(5), Article 5.https://doi.org/10.4236/oalib.1111597

Mahjoub, Y., Soualmia, A., & Kourta, A (2024b). Flood Management and Bridge Pier Designs: A Numerical Study of Dynamics in the Medjerda River. *Pioneer and innovative studies in agriculture, forest and water issues*, 23. https://www.allsciencesacademy.com/_files/ugd/13252f_1db895a8de40488fa26a154a2d1c760a.pdf#page=25

Nasim, M., Setunge, S., Zhou, S., & Mohseni, H. (2018). An investigation of water-flow pressure distribution on bridge piers under flood loading. *Structure and Infrastructure Engineering*, 15(2), 219–229. https://doi.org/10.1080/15732479.2018.1545792

Qasim, R. M., Mohammed, A. A., Abdulhussein, I. A., & Maatooq, Q. A. (2021). Experimental investigation of multi obstacles impact on weir-gate discharge structure. *International Journal of Mechatronics and Applied Mechanics*, (9), 76-84. https://doi.org/10.18280/mmep.110208

Rasha Abdulrazzak Jasim, Wajdi Qasim Hussen, Mahir Faris Abdullah, & Rozli Zulkifli. (2023). Numerical Simulation of Characterization of Hydraulic Jump Over an Obstacle in an Open Channel Flow. *Journal of Advanced Research in Fluid Mechanics and Thermal Sciences*, 106(1), 1–15. https://doi.org/10.37934/arfmts.106.1.115

Tran, D. T. (2015). Métrologie et modélisation des écoulements à forte pente autour d'obstacles : application au dimensionnement des passes naturelles (Doctoral dissertation, Institut National Polytechnique de Toulouse-INPT).

Saber Hammami, Hela Romdhane, Amel Soualmia, Azeddine Kourta. Roughness Variation Impact on the Morphological Evolution at the Medjerda River: Telemac 2D-Sisyphe Modeling. *Environment and Natural Resources Journal*, *2025*, 23 (1), pp.65-79. https://doi.org/10.32526/ennrj/23/20240043

Schlömer, O., & Herget, J. (2023). Geometry of Local Scour Holes at Boulder-like Obstacles during Unsteady Flow Conditions and Varying Submergence. *Water*, 15(5), Article 5. https://doi.org/10.3390/w15050958

Soori, S., Ikani, N., Soori, S. *et al.* (2026). Experimental investigation of three-dimensional turbulence and scour mechanisms around bridge piers and abutment using acoustic doppler velocimetry (ADV). *Environ Fluid Mech*, 26, 26, https://doi.org/10.1007/s10652-026-10087-z